AIP | Journal of Applied Physics

Analysis of field-emission from a diamond-metal-vacuum triple junction

S. Sun and L. K. Ang

Citation: J. Appl. Phys. **112**, 066102 (2012); doi: 10.1063/1.4752712
View online: http://dx.doi.org/10.1063/1.4752712
View Table of Contents: http://jap.aip.org/resource/1/JAPIAU/v112/i6
Published by the American Institute of Physics.

Related Articles

Field emission from diamond-coated multiwalled carbon nanotube “teepee” structures
J. Appl. Phys. 112, 044903 (2012)

Ultra-high current density carbon nanotube field emitter structure on three-dimensional micro-channeled copper
Appl. Phys. Lett. 101, 063110 (2012)

Shot noise of low energy electron field emission due to Klein tunneling
J. Appl. Phys. 112, 016104 (2012)

Direct observation and mechanism of increased emission sites in Fe-coated microcrystalline diamond films
J. Appl. Phys. 111, 124309 (2012)

Low threshold field emission from high-quality cubic boron nitride films
J. Appl. Phys. 111, 093728 (2012)

Additional information on J. Appl. Phys.

Journal Homepage: http://jap.aip.org/
Journal Information: http://jap.aip.org/about/about_the_journal
Top downloads: http://jap.aip.org/features/most_downloaded
Information for Authors: http://jap.aip.org/authors

ADVERTISEMENT

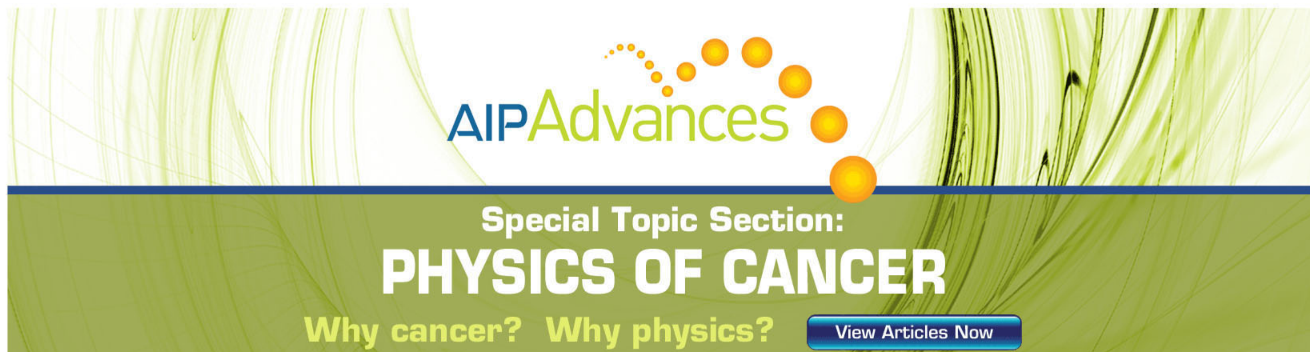

JOURNAL OF APPLIED PHYSICS 112, 066102 (2012)

Analysis of field-emission from a diamond-metal-vacuum triple junction

S. Sun[1] and L. K. Ang[1,2,a)]
[1]School of Electrical and Electronic Engineering, Nanyang Technological University, Singapore 639798
[2]Engineering Product Development, Singapore University of Technology and Design, Singapore 138682

(Received 21 May 2012; accepted 22 August 2012; published online 18 September 2012)

A quantitative electron tunneling model is constructed to calculate the electron emission from a diamond-metal-vacuum triple junction, including the effects of the field enhancement at the interface of the triple junction, the reduction on the barrier height and the negative electron affinity on the diamond surface. The difference between the emission processes with and without light exposure is also investigated. © 2012 American Institute of Physics.
[http://dx.doi.org/10.1063/1.4752712]

Diamond is known to have excellent field emission properties as compared to other semiconductors.[1] The negative electron affinity (NEA) characteristic[2,3] on the diamond surface has motivated people to investigate its field emission properties for electron to tunnel from diamond into vacuum. However, with a large band gap (5.5 eV), it is almost impossible to directly get a low turn on voltage for intrinsic diamond. To take full advantage of NEA, electrons must be present either in the conduction band or in a subband near the vacuum energy. Nevertheless, no n-type dopant suitable for cold field emission has been reported. The best choice is the substitutional nitrogen doped type Ib diamond, with nitrogen forming a deep donor level at about 1.7 eV below the conduction band.[4] Excellent low-voltage-high-current field emission had been demonstrated by using type Ib N-doped diamond and amorphous diamond-like films on metal substrates.[5–7]

An interesting experiment[8] had proposed a new mechanism combining the high electric fields at diamond-metal-vacuum triple junction[9] and the mobile electron surface states that formed on NEA surfaces.[10,11] The experimental results indicated that it can emit measurable current density (10^{-4} A/m^2) at a gate voltage as low as 0.6 V,[8] which is much smaller than the conventional diamond emitter (at about 8 to 10 V).[6] However, there is no yet quantitative model able to describe clearly the emission mechanism with comparison to experimental measurements for such a triple junction structure using type Ib diamond, which is the objective of this paper.

Before presenting our model, it is essential to review the process of electron transport from the metal substrate into the diamond layer for a traditional diamond emitter [see Fig. 1(a)]. It is generally accepted that a Schottky barrier is formed at the metal-diamond interface[6,12] as shown in Fig. 1(c) (black curve) for its corresponding band structure. Here, $\Phi_B \approx 4$ eV is the barrier height at the metal-diamond interface, which is equal to the average work function of the metal (Cs and Ni salt).[13] The deep donor level E_f is formed at 1.7 eV below the conduction band E_c for type Ib diamond ($E_c - E_f = 1.7$ eV, and E_f is assumed to be pinned with large donor concentration). The build-in potential at the junction is $V_B = V_a + V_b$, where V_a is the external applied bias and V_b is the potential difference between the peak of the Schottky barrier and the bottom of the conduction band at $V_a = 0$. Note the definition of V_a and V_b can be found in Ref. 14. At the diamond-vacuum interface, the vacuum energy E_{vac} should be below the conduction band E_c to represent the NEA characteristic, and the potential drop is determined by the surface treatment techniques used in the experiment.

Compared to the traditional diamond emitter [Fig. 1(a)], there are three major differences in the triple junction structure [Fig. 1(b)], with its corresponding band diagram depicted in Fig. 1(c) (red curve). First, in addition to the geometrical field enhancement on the metal-diamond interface due to any protrusions on the metal substrate, the local electric field at the metal-diamond-vacuum junction can be further increased by an additional factor, which is up to a value equal to the dielectric constant ($\epsilon_r = 5.68$) of the diamond.[9,15] Second, the electrons will transport into the diamond surface states at energy E_s, which is found to be 1 eV below the conduction band energy E_c given by $E_s - E_f = 0.7$ eV.[16] These electrons will face a lower barrier height $\Phi_{B1} < \Phi_B$, which could be as little as 1 eV or up to the metal work function Φ_B minus the diamond surface binding energy (0.42 eV).[8] Finally, besides the Schottky barrier $V_1(r)$ at the depletion region, there might be another barrier $V_2(r)$ formed at the diamond-vacuum interface (NEA surface) as long as $E_c > E_{vac} > E_s$.

To calculate the emission current density J, we solve

$$J = \frac{m_0 q}{2\pi^2 \hbar^3} k_B T \int_0^\infty T_c(E) \cdot \ln\left(1 + \exp\left(-\frac{E - E_f}{K_B T}\right)\right) \cdot dE, \quad (1)$$

where m_0 is the free electron mass, $\hbar$ is the reduced Plank constant, k_B is the Boltzmann constant, T is the temperature, and $T_c(E)$ is the corresponding electron tunneling coefficient through either a single barrier [$V_1(r)$] or a dual-barrier [$V_1(r)$ and $V_2(r)$][17] (see red curve in Fig. 1(c)). Note an earlier work,[14] which directly used the Fowler-Nordheim (FN) law[18] to calculate the emission current is not accurate as the potential barrier $V_1(r)$ [see Eq. (2) below] is very different from the specific potential form $V(r) = \Phi_{B1} - F \times r - Q/r$ assumed in the FN law, where Q/r is the image charge potential.

[a)]Author to whom correspondence should be addressed. Electronic mail: ricky_ang@sutd.edu.sg.

 © 2012 American Institute of Physics

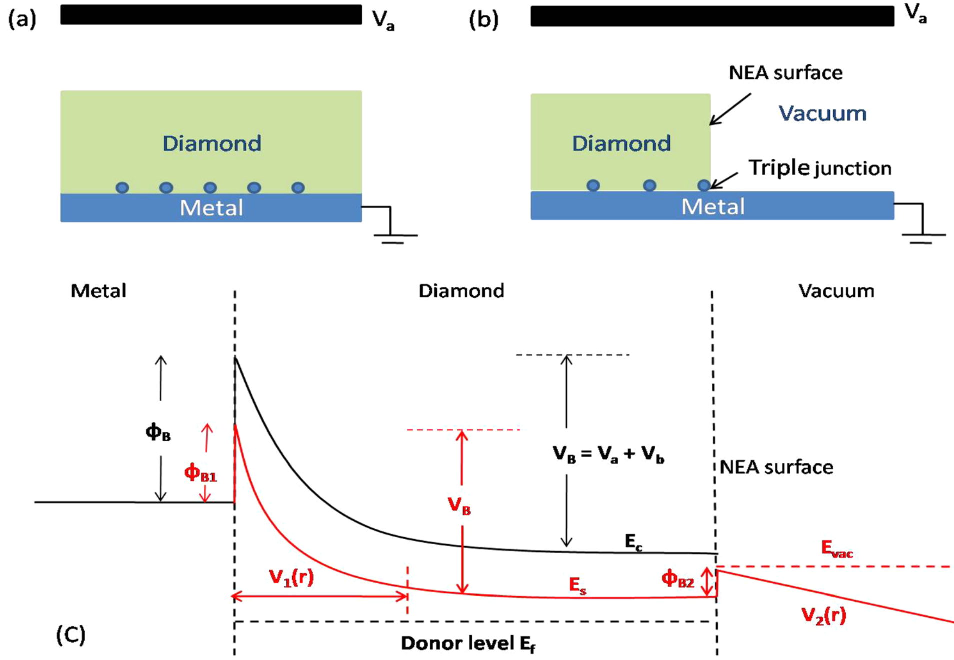

FIG. 1. (a) The schematics for a conventional diamond emitter. (b) The schematics for a triple junction structure. (c) The band diagram for a conventional diamond emitter (black curve) and a triple junction structure (red curve).

The expression of $V_1(r)$ can be derived based on prior models by considering the metal protrusive surface as spheres with radius R,[14,19,20] which give analytical expressions of

$$V_1(r) = C_1 - \frac{C_2}{r} - \frac{2\pi q N_d r^2}{3\epsilon_r \epsilon_0}, \tag{2}$$

$$C_1 = -\Phi_{B1} + \frac{2\pi q N_d R^2}{3\epsilon_r \epsilon_0} + \frac{4\pi q N_d (R+\omega)^3}{3\epsilon_r \epsilon_0 R}, \tag{3}$$

$$C_2 = \frac{4\pi q N_d (R+\omega)^3}{3\epsilon_r \epsilon_0}. \tag{4}$$

Here, $\epsilon_r = 5.68$ is the dielectric constant of diamond, ϵ_0 is the vacuum permittivity, qN_d is the charge density within the depletion layer of width ω, N_d is the donor density, and Φ_{B1} is the barrier height at the metal-diamond interface. By assuming a flat band structure far away from the barrier, we have $V_1(R+w) = V_B - \Phi_{B1}$, which can be substituted into Eq. (2) to obtain the build-in potential V_B

$$V_B = \frac{4\pi q N_d \omega^3}{3\epsilon_r \epsilon_0 R} + \frac{2\pi q N_d \omega^2}{\epsilon_r \epsilon_0}. \tag{5}$$

This equation can be used to determine the depletion width ω as a function of built-in potential V_B for fixed N_d and R. For the second barrier $V_2(r)$ at the diamond-vacuum interface, it is assumed to be $V_2(r) = \Phi_{B2} - F \times r$, where $\Phi_{B2} = E_{vac} - E_s$ is the barrier height, $F = qV_a/D$ is the average electric field, V_a is the external applied voltage, and D (=100 nm) is the diamond slab's thickness.[6]

Figure 2 demonstrates, respectively, the Schottky barrier profile $V_1(r)$ for (a) various build-in potential V_B (at $N_d = 10^{19}$ cm^{-3} and $R = 10$ nm), (b) various donor concentration N_d (at $V_B = 10$ eV and $R = 10$ nm), and (c) various metal sharpness R (at $V_B = 10$ eV and $N_d = 10^{19}$ cm^{-3}). The other parameters are $\Phi_{B1} = 3$ eV $< \Phi_B = 4$ eV, $V_b = \Phi_{B1} - (E_s - E_f) = 2.3$ eV and the metal fermi energy is kept at

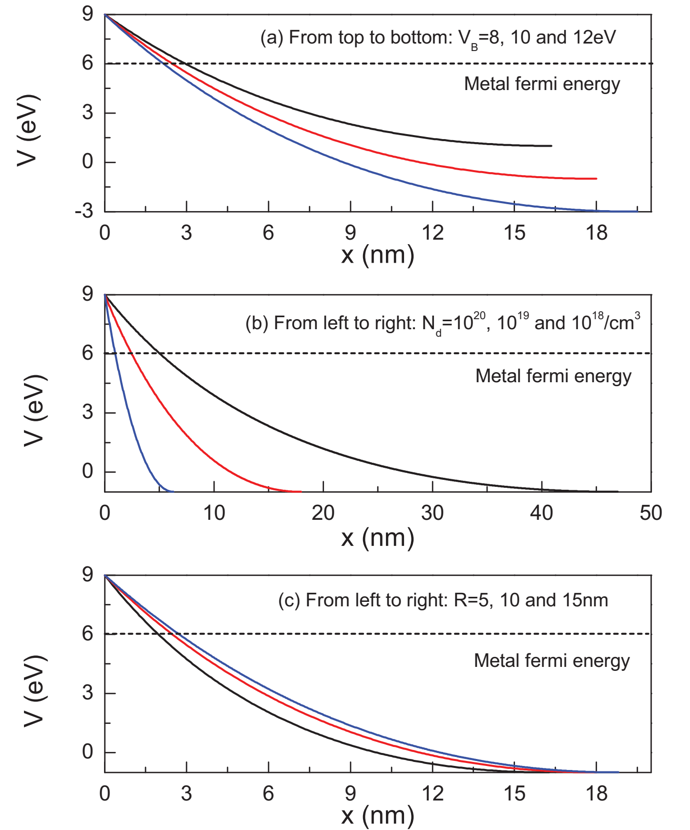

FIG. 2. (a) The Schottky barrier profile (solid lines) at different build-in potentials $V_B = 8, 10,$ and 12 eV (left to right) at $N_d = 10^{19}$ cm^{-3} and $R = 10$ nm. (b) The Schottky barrier profile (solid lines) at different donor concentrations $N_d = 10^{20}, 10^{19}$ and 10^{18} cm^{-3} (left to right) at $V_B = 10$ eV and $R = 10$ nm. (c) The Schottky barrier profile (solid lines) at different metal tip radii $R = 5$, 10, and 15 nm (left to right) at $V_B = 10$ eV and $N_d = 10^{19}$ cm^{-3}. For all the figures, metal fermi energy (dashed line) is set at 6 eV.

6 eV. By increasing V_B from 8 to 12 eV, which is equivalent to an applied voltage of $V_a(=V_B - V_b) = 5.7$ to 9.7 eV, the barrier width will become smaller, as shown in Fig. 2(a). The depletion width ω decreases with larger N_d, and increases with larger R, as shown in Figs. 2(b) and 2(c), respectively.

To compare our model with experimental results, we have used $R = 10$ nm, and the donor concentration $N_d = 10^{19}\,\mathrm{cm}^{-3}$ in order to pin the deep donor level E_f at 1.7 eV below E_c according to experimental condition.[6] In doing so, we calculate the emission current using Eq. (1) as a function of applied external voltage $V_a = V_B - V_b$, with an additional term Q/r included into the V_1 to include the image force effect, where $Q = q^2/4\pi\epsilon_r\epsilon_0$.[21]

First, without including the additional field enhancement at the triple junction[15] between metal, diamond, and vacuum, we consider only the reduction of the Schottky barrier height ($\Phi_{B1} = 3.5$ eV), and the existence of the second barrier ($\Phi_{B2} = 1$ eV) as shown in Fig. 3(a) (dashed lines), which shows that the emission current density J is about $10^{-4}\,\mathrm{A/m^2}$ at around $V_a = 5.3$ V, much smaller as compared to the conventional diamond emitter operating around 8 to 10 V with a barrier $\Phi_B \approx 4$ eV.[8] This finding proves that a smaller Schottky barrier Φ_{B1} do contribute to a smaller turn-on voltage; however, the calculated value $V_a = 5.3$ V (or electric field $F = 5.3\mathrm{V}/100\,\mathrm{nm} = 53\ \mathrm{V}/\mu\mathrm{m}$) is still significantly larger as compared to 0.6 V (or $F = 6\ \mathrm{V}/\mu\mathrm{m}$) reported in the triple junction experiment.[8]

Thus, it is rational to include the additional field enhancement factor due to triple junction, which is up to $\epsilon_r = 5.68$. By assuming an enhancement of 5, the calculated results are shown in Fig. 3(a) [solid lines] at $\Phi_{B1} = 2, 2.5$, and 3.5 eV (left to right), where V_a is decreased by a factor of 5, closer to 0.6 V. For example, we have $V_a = 1.06$ V and 0.68 V, respectively, at $\Phi_{B1} = 3.5$ eV and 2.5 eV. The emission current density is independent on the second barrier height Φ_{B2}, where the results are nearly identical for $\Phi_{B2} = 1$ eV and $\Phi_{B2} = 0.5$ eV. Hence, we conclude that the effects of field enhancement at the triple junction and the reduced Schottky barrier height Φ_{B1} are essential to get a smaller turn-on voltage to explain the experimental findings.

Lastly, we will briefly investigate the emission process with and without light exposure reported in the experiment.[8] When the cathode is exposed to light with photon energy higher than 2 eV (the ionization energy of nitrogen), the photon-generated electrons will neutralize the nitrogen dopant, which results a larger turn on voltage due to the reduction on the donor concentration. However, as the applied voltage increases, the dopant will be re-ionized recovering to the emission-in-darkness characteristic at $V_a \approx 3$ V. Since the exact relationship between the increment rate of the donor concentration N_d and the applied voltage V_a is unknown, we simply assume a linear relation governed by $N_d = 10^{19} \times (V_a/3)\,\mathrm{cm}^{-3}$ for $V_a < 3$ V, and $N_d = 10^{19}\,\mathrm{cm}^{-3}$ for $V_a \geq 3$ V in our calculation. The results are shown in Fig. 3(b), which show the difference between the emission in the darkness (solid line) and the emission in the light (dash line) at $\Phi_{B1} = 2.5$ eV. The turn-on voltage increases to 1.25 V with light exposure, which is quite comparable with the experimental data of 1.6 V.

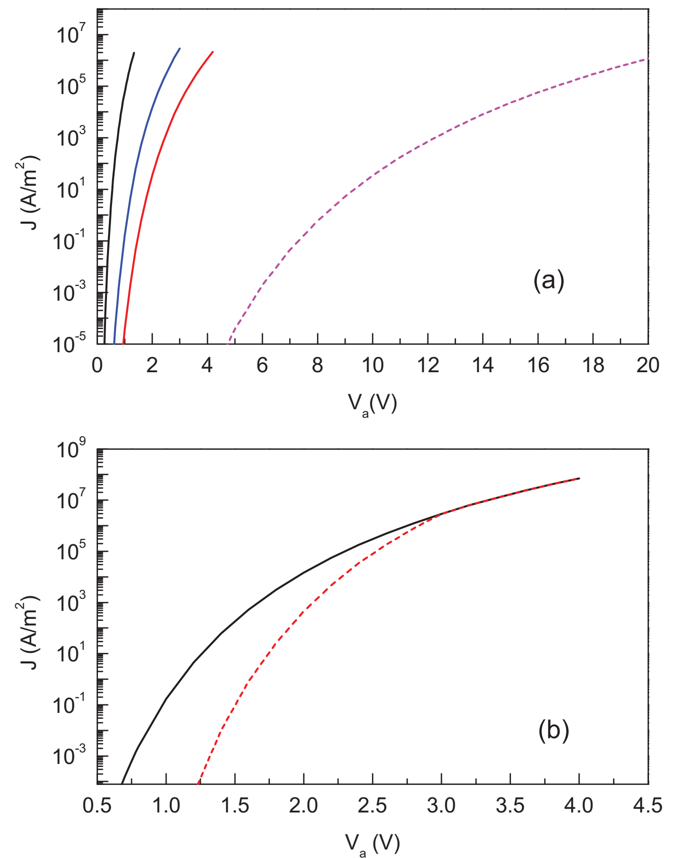

FIG. 3. (a) The emission current density with (solid lines) and without (dashed line) the additional field enhancement (=5) at the triple junction with different Φ_{B1} and fixed $\Phi_{B2} = 1$ eV. For solid lines, $\Phi_{B1} = 2, 2.5$, and 3.5 eV (left to right). For dashed line, $\Phi_{B1} = 3.5$ eV (b) The emission current density with (dashed line) and without (solid line) light exposure at $\Phi_{B1} = 2.5$ eV and $\Phi_{B2} = 1$ eV.

Our work may be extended to other triple-junction based structures or novel materials, such as graphene which has different field emission property.[22]

This work was supported by a Singapore MOE Grant (2008-T2-01-033), and USA AOARD Grant (11-4069).

[1]M. Yoder, Nav. Res. Rev. **44**(3), 17 (1992).
[2]F. J. Himpsel *et al.*, Phys. Rev. B **20**, 624 (1979).
[3]M. W. Geis *et al.*, IEEE Trans. Electron Devices **38**, 619 (1991).
[4]H. B. Dyer and L. du Preez, J. Chem. Phys. **42**, 1898 (1965).
[5]M. W. Geis *et al.*, Lincoln Lab. J. **8**, 161 (1995).
[6]M. W. Geis *et al.*, J. Vac. Sci. Technol. B **14**, 2060 (1996).
[7]K. Okana *et al.*, Nature **381**, 140 (1996).
[8]M. W. Geis *et al.*, Nature **393**, 431 (1998).
[9]C. H. D. Trourreil *et al.*, IEEE Trans. Electr. Insul. **EI-8**, 17 (1973).
[10]W. Cole, Phys. Rev. B **2**, 4239 (1970).
[11]C. C. Grimes, Surf. Sci. **73**, 379 (1978).
[12]M. W. Geis *et al.*, Appl. Phys. Lett. **68**, 2294 (1996).
[13]M. W. Geis *et al.*, Appl. Phys. Lett. **63**, 952 (1993).
[14]P. Lerner *et al.*, J. Vac. Sci. Technol. B **15**, 337 (1997).
[15]N. M. Jordan *et al.*, J. Appl. Phys. **102**, 033301 (2007).
[16]G. D. Kubiak and K. W. Kolasinski, Phys. Rev. B **39**, 1381 (1989).
[17]L. Wu and L. K. Ang, Appl. Phys. Lett. **89**, 133503 (2006).
[18]R. H. Fowler *et al.*, Proc. R. Soc. London, Ser. A **119**, 683 (1928).
[19]S. M. Sze, *Physics of Semiconductor Devices* (Wiley, New York, 1981).
[20]S. S. Li, *Semiconductor Physical Electronics* (Plenum, New York, 1993).
[21]J. He *et al.*, Surf. Sci. **246**, 348 (1991).
[22]S. Sun *et al.*, Appl. Phys. Lett. **99**, 013112 (2011).